Environ. Sci. Technol. **1999**, *33,* 2234−2240

Decomposition of Dichlorodifluoromethane by Adding Hydrogen in a Cold Plasma System

YA-FEN WANG,† WEN-JHY LEE,*,† CHUH-YUNG CHEN,‡ AND LIEN-TE HSIEH†

Department of Environmental Engineering and Department of Chemical Engineering, National Cheng Kung University, No. 1, University Road, Tainan 70101, Taiwan

The destruction of chlorofluorocarbons (CFCs) has drawn great attention because of its well-known depletion of the ozone layer at the stratosphere. Application of RF plasma for the decomposition and conversion of dichlorodifluoromethane (CFC-12 or CCl_2F_2) is demonstrated. The decomposition efficiency (η_{CFC-12}) and the fraction of total carbon input converted into CH_4 and C_2H_2 ($F_{CH_4+C_2H_2}$) in H_2 and Ar mixtures have been investigated as a function of input power wattage, H_2/CFC-12 ratio, operational pressure, and CFC-12 feeding concentration by using response surface methodology and model sensitivity analysis. The results showed that the η_{CFC-12} is over 94% and the $F_{CH_4+C_2H_2}$ is over 80% under the condition of 100 W of input power wattage, 7.0 of H_2/CFC-12 ratio, 15 Torr of operational pressure, and 7.6% of CFC-12 feeding concentration. In addition, the result of sensitivity analysis indicated that both the η_{CFC-12} and the $F_{CH_4+C_2H_2}$ are more sensitive to CFC-12 feeding concentration and input power wattage. Experimental results showed that CFC-12 could be converted into CH_4 and C_2H_2 up to 80% of conversion in a hydrogen-based RF plasma system.

Introduction

The occurrence of skin cancer increased approximately 1.5% as the amount of ozone layer decreased 1% in the stratosphere (*1*). Since 1970, the development of skin cancer increased from 15% to near 60% (*1, 2*). Chlorofluorocarbons (CFCs) were well-known man-made compounds that contributed to the depletion of the ozone layer at the stratosphere. The destruction of CFCs has drawn great attention around the world due to the stepwise forbiddance in accordance with the 1987 Montreal Protocol and subsequent revision (*3*). CFCs are, per molecule, 10 000 times more efficient in absorbing infrared radiation than carbon dioxide, and their atmospheric lifetimes fall into the range of 40−150 year (*4*). Furthermore, their stability led to rapid accumulation in the global environment and then destroyed the stratospheric ozone layer by invading the Chapman cycle (*5*). Most investigations focused on how to destroy CFCs, either by thermal technology (*6*−*9*) or catalytic method (*10, 11*). In the incineration method, the precursors of PCDD/PCDFs (polychlorodibenzo-*p*-dioxin/polychlorinated dibenzofurans) were suspected to be the products of halogenated hydrocarbons while increasing the concentration of halogen component (*12*). In catalytic method, the catalysts must be replaced frequently due to the poisoned effect by the reaction of byproducts (*10*).

Radio-frequency (RF) plasma is a branch of nonequilibrium plasma that is often referred to as cold plasma (*13*). The temperature of the gas molecule in an RF plasma reactor is near room temperature, while the temperature of electrons will be higher than 10^4 K. At such high temperature, the energy of an electron is much higher than 200 kJ mol^{-1}. It is two times magnitude higher than the activation energy of a conventional chemical reaction (100 kJ mol^{-1}) (*14*). The kinetic energy of electrons and ions is much higher than that of molecules in the cold plasma system. Therefore, the conventional reaction, which needs to proceed at a very high temperature, can be finished at lower temperature in the cold plasma system (*15*−*17*). The coexistence of warm gas and high-temperature active species distinguishes the plasma system from conventional thermal processing (*18*). Besides, RF plasma is free from electrode erosion by byproducts such as HCl or HF or spark problem while comparing with DC plasma or pulsed corona (*19, 20*).

In this study, CFC-12 and H_2 mixtures were introduced into the RF plasma reactor with an operational pressure of 15 Torr. In contrast with the previous studies (*7*−*10*), this work concentrated on not only the CFC-12 decomposition but also on the conversion of the carbon on CFC-12 into methane (CH_4) and acetylene (C_2H_2). In addition, the fractional factorial design (*21*) was employed in planning the experiments for studying the effects of experimental variables on the CFC-12 decomposition efficiency (η_{CFC-12}) and the fraction of total carbon input converted into CH_4 and C_2H_2 ($F_{CH_4+C_2H_2}$). Furthermore, the results of experiments were subjected to regression analysis to determine the conditions required for a better η_{CFC-12} and a higher $F_{CH_4+C_2H_2}$.

Experimental Apparatus

The experimental apparatus used in this study is schematically shown in Figure 1. The CFC-12/H_2/Ar mixing gas was metered using Tylan type 1179 mass flow controllers at a total flow rate of 100 standard cm^3/min that were entered, then directed to a mixing vessel, and introduced perpendicularly into a 4.14 × 15 cm cylindrical glass reactor. The RF plasma discharge was produced using a plasma generator (PFG 600 RF, Fritz Huttinger Elektronik Gmbh) at 13.56 MHz and with a matching network (Matchbox PFM). RF power was delivered through the power meter and the matching unit to an outer copper electrode wrapped on the reactor with another electrode earthed.

Before the experiment, a diffusion pump was used to keep the system pressure lower than 0.001 Torr for the cleanup of contamination. For each designed experimental condition [the input power wattage (factor A), the H_2/CFC-12 ratio (B), the operational pressure (C). and the CFC-12 feeding concentration (D)] were measured more than three times within a 5-min period in order to ensure that steady-state conditions were achieved. The reactants and final products were identified by gas chromatography/mass spectrometry (Varian Saturn 2000 GC/MS) first and then identified and quantified by an on-line Fourier transform infrared (FTIR) spectrometer (Bio-Rad, Model FTS-7).

The reactants and products were sampled from the outlet valve downstream from the plasma reactor through a canister sampler (Figure 1). The collected gas was separately injected into the GC/MS and the GC/FID (gas chromatography/flame ionization detector) systems by thermal desorption apparatus. Chlorofluorocarbons were analyzed by the GC/MS,

* Corresponding author telephone: 886-6-275-7575, ext 54531; fax: 886-6-275-2790; e-mail: wjlee@mail.ncku.edu.tw.
† Department of Environmental Engineering.
‡ Department of Chemical Engineering.

10.1021/es980757e CCC: $18.00
Published on Web 05/13/1999

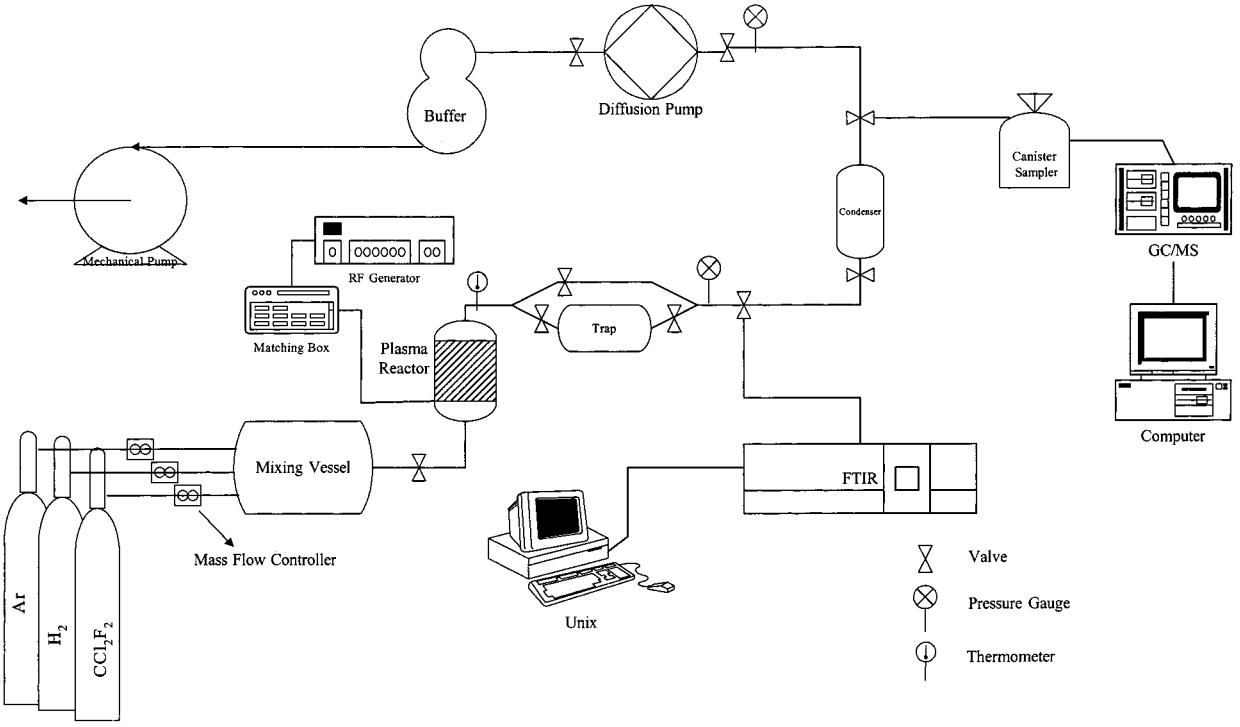

FIGURE 1. Schematic of the RF plasma system.

TABLE 1. Factors and Levels for the 2^{4-1} Fractional Factorial Design

factors	levels +	levels −
A: input power wattage (W)	120	50
B: H_2/CFC-12 ratio	2.0	0.5
C: operational pressure (Torr)	20	10
D: CFC-12 feeding concentration (%)	15	8.0

while hydrocarbons were analyzed by the GC/FID. Calibration of gaseous reactants and products was made by withdrawing unreacted gases and by going directly through the sampling line connected to the FTIR. The mass of species was calculated by comparing the response factor (absorbance height/concentration) of standard gas at the same IR wavenumber. To understand the significance of deposition and condensation that occurred in the sampling and analyzing system, the FTIR quantification data were also checked through carbon balance.

Results and Discussion

Fractional Factorial Design. The fractional factorial design method and response surface procedure were established in order to identify the key variables in influencing the η_{CFC-12} and the $F_{CH_4+C_2H_2}$. The design of factors and levels for the first 2^{4-1} fractional factorial experiments are listed in Table 1. The η_{CFC-12} was higher than 90% when the input power wattage was higher than 100 W; therefore, a higher input power wattage (factor A), 120 W, was chosen. Soot formation and white deposition led to the decreasing of carbon balance becoming apparent when the H_2/CFC-12 ratio moved away from 2.0. Accordingly, the high level of factor B was chosen as 2.0. Dimmer plasma was found at the operational pressure higher than 20 Torr, which was chosen as the high level in Table 1. The 15% of factor D was chosen as the high level due to serious soot formation when the CFC-12 feeding concentration was higher than 15%. The η_{CFC-12} and the $F_{CH_4+C_2H_2}$ were defined as follows: η_{CFC-12}: CFC-12 decomposition efficiency (%)

$$= [(C_{in} - C_{out})/(C_{in})] \times 100\% \quad (1)$$

C_{in}: the feeding concentration of CFC-12 (%) C_{out}: the effluent concentration of CFC-12 (%) $F_{CH_4+C_2H_2}$ (%): the fraction of total carbon input converted into CH_4 and C_2H_2 (%)

$$= [C_{CH_4+C_2H_2}/C_{in}] \times 100\% \quad (2)$$

$C_{CH_4+C_2H_2}$: the effluent concentration of CH_4 and C_2H_2 (%).

Estimates of the experimental variable effects were calculated following the procedure recommended by Box et al. (*21*), and the results are given in Table 2. According to the basic assumption of Box et al., higher order interaction effects (above three-factor interaction) being often negligible and ignored, the results of Table 2 reveal that the input power wattage (A) and CFC-12 feeding concentration (D) were the key variables by contrast with other factors and that interaction effects did not matter for the η_{CFC-12} or the $F_{CH_4+C_2H_2}$. To quantitatively elucidate the effects of all study variables, the results of fractional factorial design were subjected to regression analysis. The analysis generated the following equations:

$$\eta_{CFC-12} = 61.57 + 11.48A - 7.62B - 8.98C - 18.30D \quad (R^2 = 0.89) \quad (3)$$

TABLE 2. Estimates of the Effects from the 2^{4-1} Fractional Factorial Design with the Defining Relation $I = ABCD$

effects	estimate (η_{CFC-12})	estimate ($F_{CH_4+C_2H_2}$)
*A + BCD	22.95	26.36
B + ACD	−15.24	16.73
C + ADB	−17.95	−7.33
*D + ABC	−36.59	−27.09
AB + CD	−9.15	2.13
AC + BD	−14.49	−13.08
AD + BC	−2.73	9.25

$$F_{CH_4+C_2H_2} = 49.57 + 13.18A + 8.36B - 3.66C - 13.55D \quad (R^2 = 0.87) \quad (4)$$

Model Sensitivity Analysis. The aim of model sensitivity analysis was to gain a better insight into the relative importance of the various experimental variables for the plasma reactor. The sensitivity of this model changing in the four model variables (A−D) has been tested. Estimates of the model sensitivity analysis were calculated following the procedure recommended by Hsieh et al. (*22*), and the results are given in Figure 2. The absolute significance of sensitivity for η_{CFC-12} was D > A > C > B, and that for $F_{CH_4+C_2H_2}$ was D > A > B > C. Both the η_{CFC-12} and the $F_{CH_4+C_2H_2}$ were more sensitive to the CFC-12 feeding concentration. The results were coincident with that of Table 2. Lower CFC-12 feeding concentration and higher input power wattage will lead to a higher η_{CFC-12} and a higher $F_{CH_4+C_2H_2}$.

Path of Steepest Ascent and Central Composite Design. Equations 3 and 4 represent the experimental data as a first-order model. Additional experiments were conducted to evaluate A, B, and D via the path of steepest ascent methodology (*21*). The H_2/CFC-12 ratio (factor B) was added into the methodology due to taking the $F_{CH_4+C_2H_2}$ into account. On the basis of the results of the path of steepest ascent, 16 central composite designs were performed to investigate the relationship among the η_{CFC-12}, the $F_{CH_4+C_2H_2}$, the input power wattage, the H_2/CFC-12 ratio, and the CFC-12 feeding concentration. The results of central composite design were also subjected to regression analysis and generated the following equation (substituting D = −1 owing to a higher CFC-12 feeding concentration will lead to more soot formation):

$$\eta_{CFC-12} = 98.07 + 2.20A + 2.39B - 0.92A^2 - 1.05B^2 - 1.90AB \quad (R^2 = 0.99) \quad (5)$$

$$F_{CH_4+C_2H_2} = 88.00 + 1.88A + 1.36B - 0.83A^2 - 0.54B^2 - 1.38AB \quad (R^2 = 0.92) \quad (6)$$

According to the procedure recommended by Box et al. (*21*), a higher η_{CFC-12} will be achieved between 95 and 125 W of input power wattage and between 0.5 and 3.0 H_2/CFC-12 ratio. In addition, a higher $F_{CH_4+C_2H_2}$ will be achieved between 85 and 115 W of input power wattage and between 1.0 and 3.5 H_2/CFC-12 ratio. The following experiments were performed under the designed experimental variables; Ar was used as carrier gas; the combination of experimental variables was 100 W of input power wattage, 7.0 of H_2/CFC-12 ratio, 15 Torr of operation pressure, 7.6% of CFC-12 feeding concentration, and 100 standard cm^3 of total gas flow rate. The choice of higher H_2/CFC-12 ratio will form a preferential pathway for the formation of HCl and HF, which are thermodynamically stable diatomic species that limit the production of other chlorine- and fluorine-containing compounds. A steady state was considered to be reached when relatively constant values of both decomposition efficiencies and the absorbance peaks of product species on FTIR were obtained at designed experimental variables. Each run of experiment lasted for 20 min, and the effluent concentration of individual species was monitored by FTIR and confirmed by GC/MS. The major products from the reaction of CFC-12 and H_2 were CH_4, C_2H_2, HCl, HF, and SiF_4. The formation of SiF_4 was due to the well-known plasma−chemical etch reaction: Si + 4F + ion bombardment → SiF_4 (*23*). The SiF_4 can be converted into CaF_2 according to the results proposed by Breitbarth et al. (*24*). In addition, the HCl and HF were easily removed by scrubbing or neutralizing (*25*).

Soot and Deposition. A lower H_2/CFC-12 ratio (<3.3) and a higher CFC-12 feeding concentration (>7.6%) will lead to the formation of soot. Analysis of soot showed that the summation of 21 PAHs (polycyclic aromatic hydrocarbons) content was about 1030 μg/g. The naphthalene, benzo[*b*]-chrysene, and coronene were dominant in this collected soot; their concentrations were 472, 168, and 101 μg/g, respectively. These 21 PAHs and the analytic procedure for the PAHs were the same as a previous study (*26*). Zhu et al. (*27*) pointed out that the consecutive addition and cyclization of hydrocarbon free radical will lead to the PAHs formation. In addition, there was white film deposition formed on the inside and downstream of the plasma reactor. The result of electron spectroscopy for chemical analysis (ESCA, ESCA-210) analysis showed that there was carbon, fluorine, and silicon involved in the deposition. The formation of soot and deposition will lead to a decrease of carbon balance during the experiments. Furthermore, the polymerization process in Ar (without H_2) plasma is mainly propagated by an ion−molecule mechanism, while addition of H_2 to the Ar plasma propagates the polymerization chiefly by a radical mechanism (*28*). The results of photographs for scanning electron microscopy (SEM, JXA840A) with and without Ar involved showed that the smaller and denser crystals were formed with a higher amount of H_2 input (Figure 3).

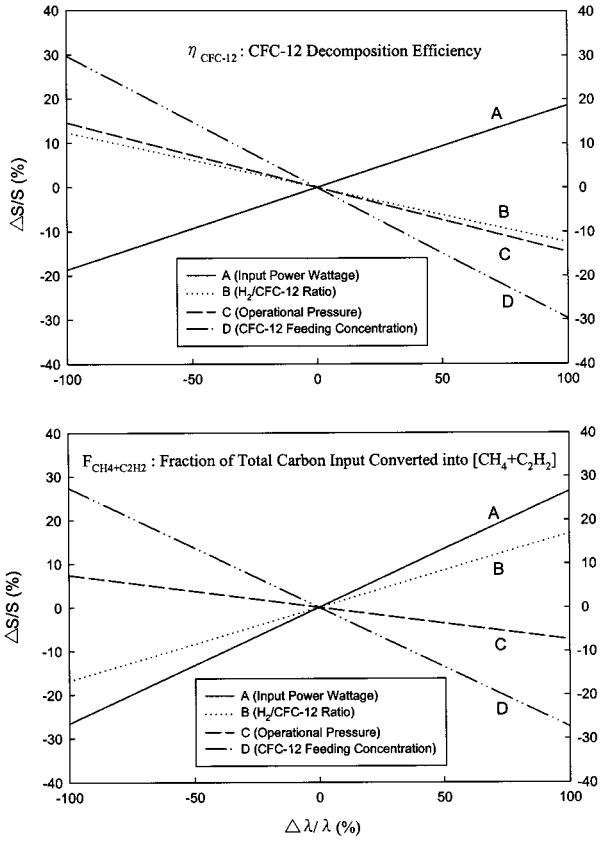

FIGURE 2. Model sensitivity analysis for the CFC-12 decomposition efficiency and fraction of total carbon input converted into [CH_4 + C_2H_2].

Input Power Wattage. Experiments were conducted to determine the dependence of η_{CFC-12} and $F_{CH_4+C_2H_2}$ on the input power wattage ranging from 35 to 110 W with the H_2/CFC-12 ratio as 7.0, the operational pressure as 15 Torr, and the CFC-12 feeding concentration as 7.6%. Figure 4A showed that the carbon balance decreased with the increasing input power wattage in the reactor. This was due to the formation of deposition on the inner walls of both the plasma reactor and the trap in contact with flue gas under CFC-12/H_2/Ar plasma. Figure 4B showed that the mole fractions of HCl and HF increased respectively with the increasing input power wattage. A higher input power wattage will provide more

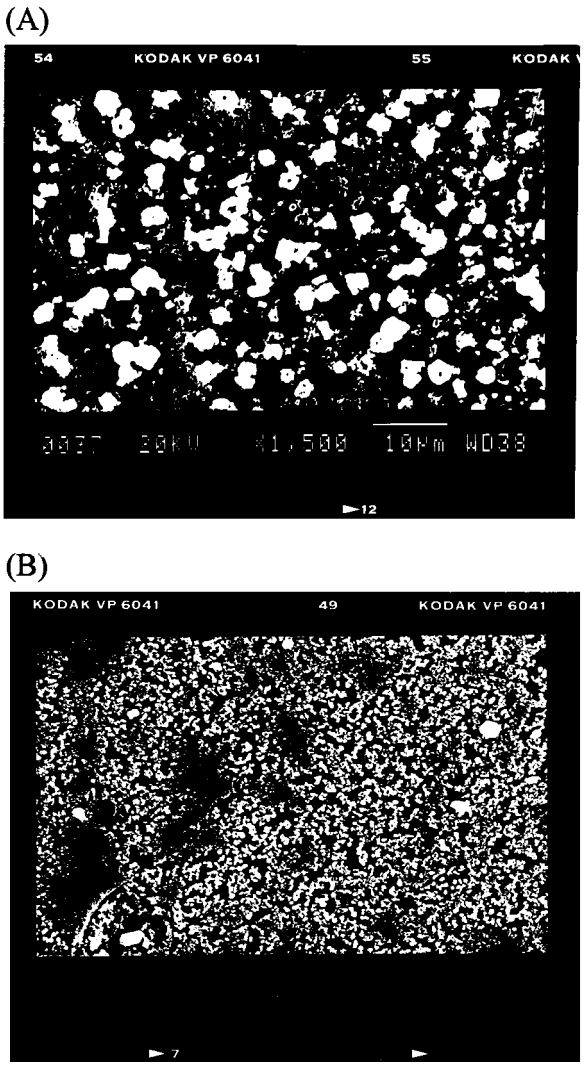

FIGURE 3. (A) Deposition with Ar involved. (B) Deposition without Ar involved.

energy to the reactor under the same discharge time, which will result in the elevation of temperature of reaction. In addition, the etch reaction rate constant was proportional to the plasma power input due to etch process being plasma activated. The mole fraction of SiF_4 also increased with the increasing input power wattage. Figure 4C,D showed that the η_{CFC-12} and the $F_{CH_4+C_2H_2}$ increased as the input power wattage increased. Furthermore, the fraction of total carbon input converted into CH_4 (F_{CH_4}) and the fraction of total carbon input converted into C_2H_2 ($F_{C_2H_2}$) also increased as the input power wattage increased. Higher input power wattage resulting in higher temperature will spread out the Maxwell−Boltzmann velocity distribution to higher speeds and therefore to higher energies (*29, 30*). Consequently, energetic species and effective collision frequency among reactants were increased and resulted in a higher η_{CFC-12}, F_{CH_4}, $F_{C_2H_2}$, and $F_{CH_4+C_2H_2}$.

H_2/CFC-12 Ratio. Experiments were conducted to determine the dependence of η_{CFC-12} and $F_{CH_4+C_2H_2}$ on the H_2/CFC-12 ratio ranging from 0.7 to 12.2 with the input power wattage as 100 W, the operational pressure as 15 Torr, and the CFC-12 feeding concentration as 7.6%. There was no argon involved when the H_2/CFC-12 ratio was at 12.2. Figure 5A showed that carbon balance increased at first and then decreased for the H_2/CFC-12 ratio from 2.0 to 12.2. Soot formation became apparent when the H_2/CFC-12 ratio was lower than 2.0, while the deposition became thicker when

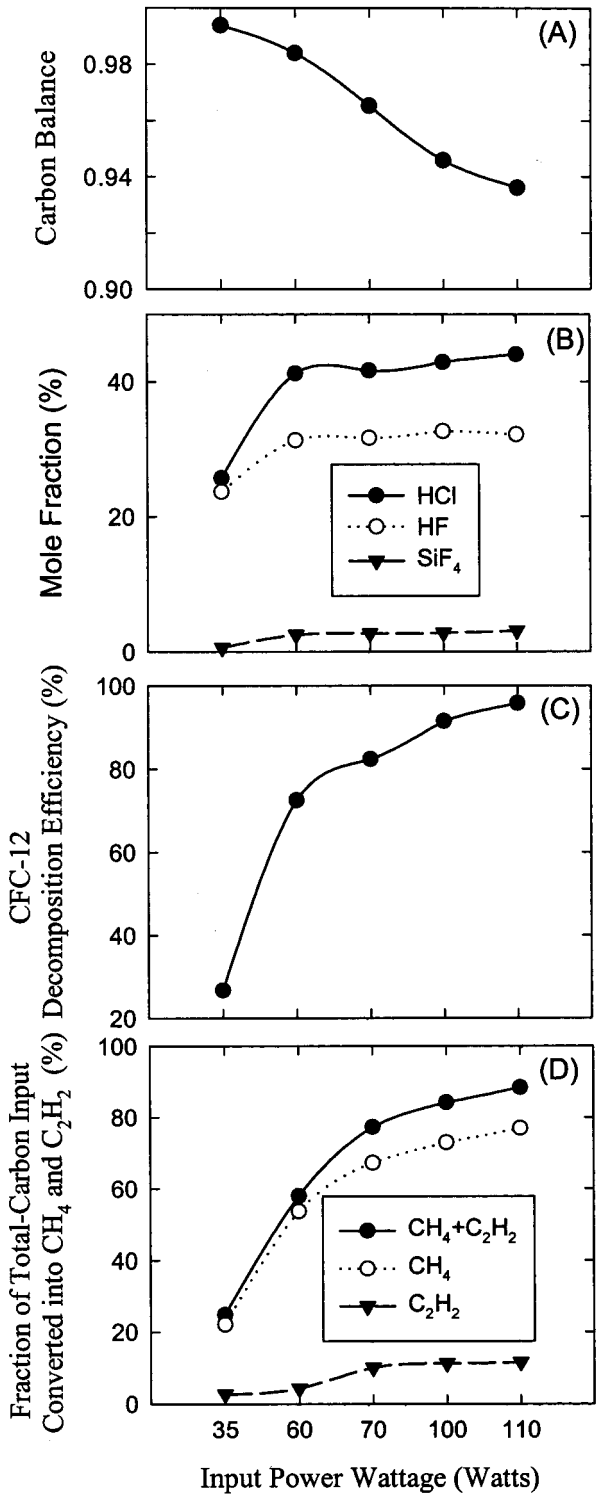

FIGURE 4. (A) Carbon balance. (B) Mole fraction of HCl, HF, and SiF_4 (%). (C) η_{CFC-12} (%). (D) $F_{CH_4+C_2H_2}$ (%) in the various input power wattages.

the H_2/CFC-12 ratio was higher than 3.3. These will both lead to the decreasing of the carbon balance. Figure 5B showed that the mole fraction of HCl decreased as the H_2/CFC-12 ratio increased, while that of HF increased as the H_2/CFC-12 ratio increased. A higher amount of H_2 addition will enhance the polymerization rather than etching (*23*). This led to the decreasing of SiF_4 as the H_2/CFC-12 ratio increased from 0.7 to 12.2. The dependence of η_{CFC-12} on H_2/CFC-12 ratio was shown in Figure 5C. The result indicated that η_{CFC-12} reached near 100% for the H_2/CFC-12 ratio

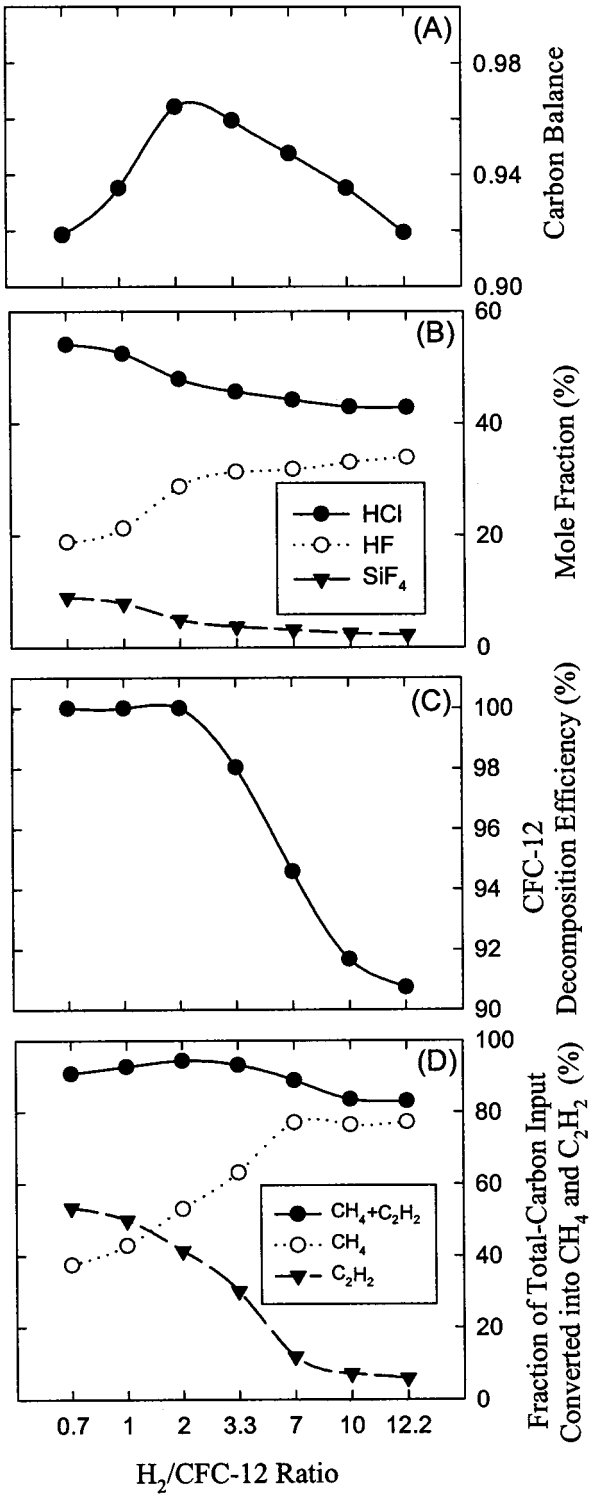

FIGURE 5. (A) Carbon balance. (B) Mole fraction of HCl, HF, and SiF_4 (%). (C) η_{CFC-12} (%). (D) $F_{CH_4+C_2H_2}$ (%) in the various H_2/CFC-12 ratios.

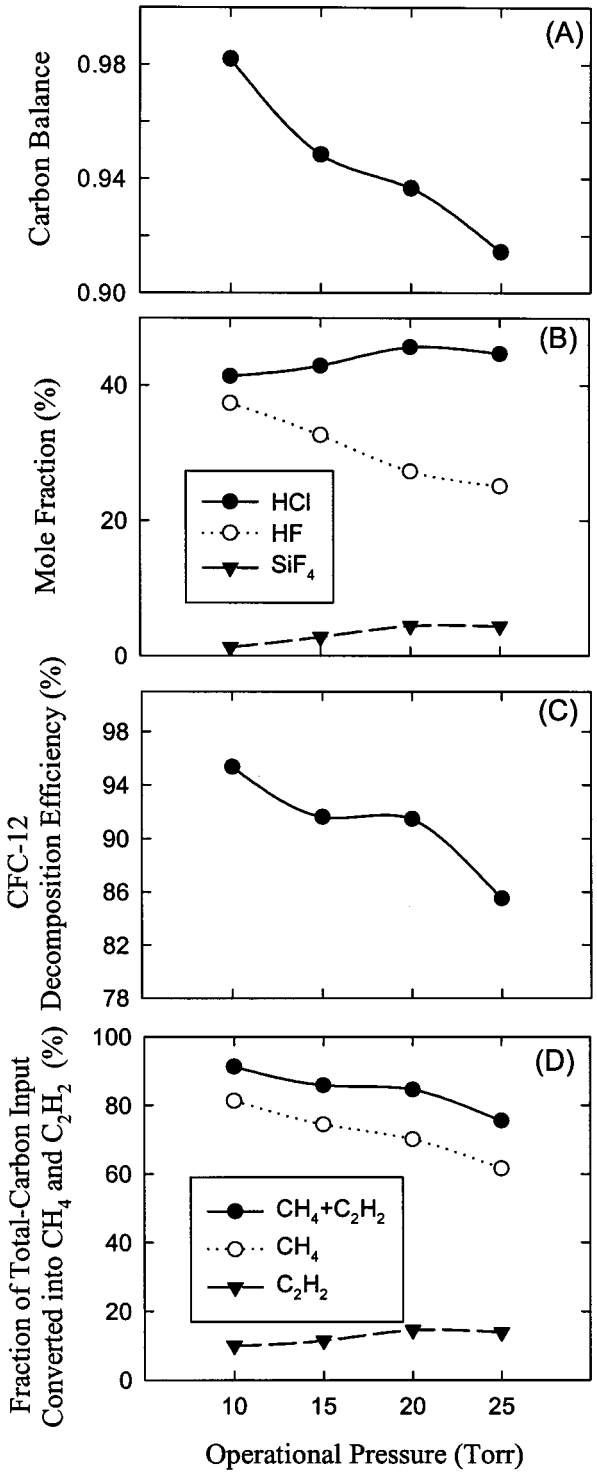

FIGURE 6. (A) Carbon balance. (B) Mole fraction of HCl, HF, and SiF_4 (%). (C) η_{CFC-12} (%). (D) $F_{CH_4+C_2H_2}$ (%) in the various operational pressures.

between 0.7 and 2.0, while that decreased to 90.7% when the H_2/CFC-12 ratio was at 12.2. The addition of more hydrogen into the plasma reactor inhibited the values of both mean electron energy and positive ion density (*28*) and then resulted in a lower η_{CFC-12}. Figure 5D showed that the $F_{CH_4+C_2H_2}$ reached maximum when the H_2/CFC-12 ratio was 2.0, whereas F_{CH_4} increased as the H_2/CFC-12 ratio increased and $F_{C_2H_2}$ decreased as the H_2/CFC-12 ratio increased. A lower H_2/CFC-12 ratio along with a higher Ar concentration will increase the probability to convert the produced CH_4 into more stable C_2H_2 (*22*). Hence, a lower amount of CH_4 and a higher amount of C_2H_2 were formed due to the stronger attacking capability of increasing concentration of excited Ar* at a lower H_2/CFC-12 ratio.

Operational Pressure. Experiments were conducted to determine the dependence of η_{CFC-12} and $F_{CH_4+C_2H_2}$ on the operational pressure ranging from 10 to 25 Torr with the input power wattage as 100 W, the H_2/CFC-12 ratio as 7.0, and the CFC-12 feeding concentration as 7.6%. No soot formation was found in the plasma reactor under the various operational pressure. The result of Figure 6A showed that

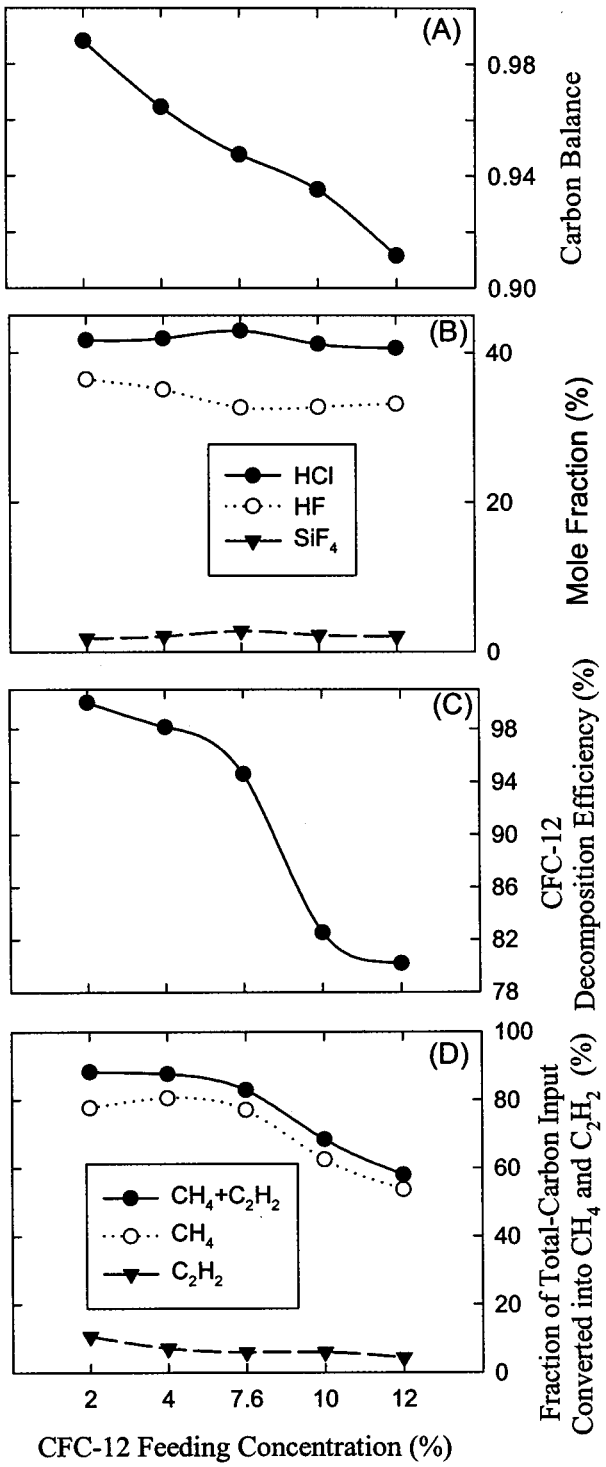

FIGURE 7. (A) Carbon balance. (B) Mole fraction of HCl, HF, and SiF_4 (%). (C) η_{CFC-12} (%). (D) $F_{CH_4+C_2H_2}$ (%) in the various CFC-12 feeding concentrations.

the carbon balance decreased when the operational pressure increased. Thicker deposition was produced as the operational pressure increased and resulted in a lower carbon balance. The dependence of mole fractions of HCl, HF, and SiF_4 on operational pressure was shown in Figure 6B. The results showed that there was little change for the mole fractions of HCl and SiF_4 respectively when the operational pressure was between 10 and 25 Torr. An increase in pressure will shift the electron-energy distribution to lower values and will thus reduce the rate constant for inelastic collision (*29*, *30*). This will lead to the decreasing of η_{CFC-12}, which is shown in Figure 6C. Figure 6D indicated that $F_{CH_4+C_2H_2}$ and F_{CH_4} both decreased with the increasing operational pressure but that $F_{C_2H_2}$ increased with the increasing operational pressure. The inductively coupled system with external electrode and conductive plasma inside the reactor will develop a negative self-bias (*23*). Under the same input power wattage, a lower operational pressure will develop a higher self-bias and then result in a stronger electric field. An increasing efficiency of energy transfer will lead to a higher amount of CH_4 formation (*22*).

CFC-12 Feeding Concentration. Experiments were conducted to determine the dependence of η_{CFC-12} and $F_{CH_4+C_2H_2}$ on the CFC-12 feeding concentration ranging from 2% to 12% with the input power wattage as 100 W, the H_2/CFC-12 ratio as 7.0, and the operational pressure as 15 Torr. Figure 7A showed that, at the CFC-12 feeding concentration higher than 7.6%, little soot formation and polymerization were found in the plasma reactor, which resulted in a lower carbon balance. In addition, the result of Figure 7B showed that the mole fractions of HCl and SiF_4 increased as the CFC-12 feeding concentration was between 2% and 7.6%. More reactants and higher fluorine atom concentration will elevate the production of HCl and SiF_4. However, the mole fraction of HF decreased with the increasing CFC-12 feeding concentration. This was possibly due to the competition reaction between H−F and Si−F bonds. The dependence of η_{CFC-12}, $F_{CH_4+C_2H_2}$, F_{CH_4}, and $F_{C_2H_2}$ on various CFC-12 feeding concentrations is shown in Figure 7C,7D. The η_{CFC12}, $F_{CH_4+C_2H_2}$, F_{CH_4}, and $F_{C_2H_2}$ all decreased with increasing CFC-12 feeding concentration. Increasing the CFC-12 feeding concentration will result in a higher molecule density, a lower concentration of excited Ar*, and a reduced mean free path between reactants' collision. This will all lead to a lower η_{CFC-12} and a lower $F_{CH_4+C_2H_2}$ (*22*).

This study demonstrates the possibility of converting CFC-12 into CH_4 and C_2H_2. With the addition of excess hydrogen, not only was the CFC-12 almost decomposed but also more than 80% of $F_{CH_4+C_2H_2}$ was achieved. The η_{CFC-12} and the $F_{CH_4+C_2H_2}$ are more sensitive to the input power wattage and the CFC-12 feeding concentration than that of H_2/CFC-12 ratio and operational pressure. In general, increasing the input power wattage will increase both η_{CFC-12} and $F_{CH_4+C_2H_2}$, while increasing the operational pressure and the CFC-12 feeding concentration will decrease both η_{CFC-12} and $F_{CH_4+C_2H_2}$. Applying RF plasma along with the addition of hydrogen has provided an alternative for converting CFC-12 into CH_4 and C_2H_2.

Acknowledgments

The research was supported by funds from National Science Council, Taiwan, Grant NSC 87-2218-E-006-067.

Literature Cited

(1) Madronich, S.; De Gruijl, F. R. *Nature* **1993**, *366*, 23.
(2) De Fabo, E. C.; Noonan, F. P. *Int. J. Environ. Stud.* **1996**, *51*, 257−268.
(3) Ad-Hoc Technical Advisory Committee on ODS Destruction Technologies, Environ. Programme, United Nations, May 1992.
(4) Rowland, F. S. *Am. Sci.* **1989**, *77*, 36−45.
(5) Finlayson-Pitts, B. J.; Pitts, J. N., Jr. *Atmospheric Chemistry*; John Wiley & Sons: New York, 1986.
(6) Sekiguchi, H.; Honda, T.; Kanzawa, A. *Plasma Chem. Plasma Process.* **1993**, *13*, 463−478.
(7) Penetrante, B. M.; Schultheis, S. E. *Non-Thermal Plasma Techniques for Pollution Control.* NATO ASI Series G, Ecological Sciences, Vol. 34, Part A; NATO: 1993.
(8) Tokuhashi, K.; Urano, Y.; Horiguchi, S.; Kondo, S. *Combust. Sci. Technol.* **1990**, *72*, 117−129.
(9) Ueno, H.; Iwasaki, Y.; Tatsuichi, S.; Soufuku, M. *J. Air Waste Manage. Assoc.* **1997**, *47*, 1220−1223.
(10) Aida, T.; Higuchi, R.; Niiyama, H. *Chem. Lett.* **1990**, 2247−2250.

(11) Sonoyama, N.; Sakata, Y. *Environ. Sci. Technol.* **1998**, *32*, 375−378.
(12) Rittmeyer, C.; Kaese, P.; Vehlow, J.; Vilöhr, W. *Chemosphere* **1994**, *28*, 1455−1465.
(13) Eliasson, B.; Kogelschatz, U. *IEEE T. Plasma Sci.* **1991**, *19*, 1063−1077.
(14) Hsieh, L. T.; Lee, W. J.; Li C. T.; Chen, C. Y.; Wang, Y. F.; Chang, M. B. *J. Chem. Technol. Biotechnol.* **1998**, *73*, 432−442.
(15) Lee, W. J.; Chen, C. Y.; Lin, W. C.; Wang, Y. T.; Chin, C. J. *J. Hazard. Mater.* **1996**, *48*, 51−67.
(16) Li, C. T.; Lee, W. J.; Chen, C. Y.; Wang, Y. T. *J. Chem. Technol. Biotechnol.* **1996**, *66*, 382−388.
(17) Hsieh, L. T.; Lee, W. J.; Chen, C. Y.; Wu, Y. P. Greg.; Chen, S. J.; Wang, Y. F. *J. Hazard. Mater.* **1998**, *B63*, 69−90.
(18) Manos, D. M.; Flamm, D. L. *Plasma Etching: An Introduction*: Academic Press: New York, 1989.
(19) Chang, J. S. *Proceeding of The First Asia-Pacific International Symposium on the Basic and Application of Plasma Technology;* December 15−16, 1997; pp 11−18.
(20) Penetrante, B. M.; Schultheis, S. E. *Non-Thermal Plasma Techniques for Pollution Control;* NATO ASI Series G, Ecological Sciences, Vol. 34, Part B; NATO: 1993.
(21) Box, G. E. P.; Hunter, W. G.; Hunter, J. S. *Statistics for Experiments*; John Wiley & Sons: New York, 1978.
(22) Hsieh, L. T.; Lee, W. J.; Chen, C. Y.; Chang, M. B.; Chang, H. C. *Plasma Chem. Plasma Process.* **1998**, *18*, 215−239.
(23) Biederman, H.; Osada, Y. *Plasma Polymerization Processes*; Elsevier Science: New York, 1992.
(24) Breitbarth, F. W.; Berg, D.; Dumke, K.; Tiller, H.-J. *Plasma Chem. Plasma Process.* **1997**, *17*, 39−57.
(25) Hartz, C. L.; Bevan, J. W.; Jackson, M. W.; Wofford, B. A. *Environ. Sci. Technol.* **1998**, *32*, 682−687.
(26) Sheu, H. L.; Lee, W. J.; Su, C. C.; Chao, H. R.; Fan, Y. C. *J. Environ. Eng. ASCE* **1996**, *122*, 1101−1109.
(27) Zhu, M.; Miao, Q.; Parulekar, S. J. *Chem. Eng. Sci.* **1992**, *47*, 2677−2682.
(28) Boenig, H. *Fundamentals of Plasma Chemistry and Technology*; Technomic Publishing Co.: Lancaster, PA, 1988.
(29) Roth, J. R. *Industrial Plasma Engineering, Volume 1: Principles;* Institute of Physics: Bristol and Philadelphia, 1995.
(30) Chapman, B. *Glow Discharge Processes*; John Wiley & Sons: New York, 1980.

Received for review July 23, 1998. Revised manuscript received March 16, 1999. Accepted March 26, 1999.

ES980757E